

Metal–Metal Bonded Diruthenium Unit Axial-Capped by Di-*tert*-butylphenolate: $[Ru_2(O_2CCH_3)_2(t\text{-Busal-R}'py)_2]^-$ (t-Busal-R′py^{2-} = *N*-(R′-2-pyridyl)-2-oxido-3,5-di-*tert*-butylbenzylaminato; R′ = H, 4-Me, and 5-Me)

Hitoshi Miyasaka,*[1] Toru Izawa,[1] Shinya Takaishi,[2] Kunihisa Sugimoto,[3] Ken-ichi Sugiura,[1] and Masahiro Yamashita[2]

[1]Department of Chemistry, Graduate School of Science, Tokyo Metropolitan University, 1-1 Minamiohsawa, Hachioji, Tokyo 192-0397

[2]Department of Chemistry, Graduate School of Science, Tohoku University, 6-3 Aoba, Aramaki, Aoba-ku, Sendai 980-8578

[3]X-ray Research Laboratory, Rigaku Co., Ltd., 3-9-12 Matsubara-cho, Akishima, Tokyo 196-8666

Received October 20, 2005; E-mail: miyasaka@comp.metro-u.ac.jp

Three diruthenium compounds, $[Na(18\text{-crown-6})(thf)_2][Ru_2(O_2CCH_3)_2(t\text{-Busalpy})_2]$ (**1**), $[K(18\text{-crown-6})(thf)_2][Ru_2(O_2CCH_3)_2(t\text{-Busal-4-Mepy})_2]$ (**2**), and $[K(18\text{-crown-6})(thf)(H_2O)][K(18\text{-crown-6})(thf)(MeO)][Ru_2(O_2CCH_3)_2(t\text{-Busal-5-Mepy})_2]$ (**3**) (18-crown-6 = 1,4,7,10,13,16-hexaoxocyclooctadecane; 18-crown-6-ether), have been synthesized by the ligand substitution reaction of $Ru_2(O_2CCH_3)_4Cl$ with newly prepared tridentate bridging/chelating ligands, *N*-(2-pyridyl)-2-oxido-3,5-di-*tert*-butylbenzylaminato (t-Busalpy^{2-}), *N*-(4-methyl-2-pyridyl)-2-oxido-3,5-di-*tert*-butylbenzylaminato (t-Busal-4-Mepy^{2-}), and *N*-(5-methyl-2-pyridyl)-2-oxido-3,5-di-*tert*-butylbenzylaminato (t-Busal-5-Mepy^{2-}), respectively, and isolated using $[Na(18\text{-crown-6})]^+$ or $[K(18\text{-crown-6})]^+$ as the counter cation. The structural features of the anionic parts are very similar to those of the previously synthesized family of $[Ru_2(O_2CCH_3)_2(5\text{-Rsalpy})_2]^-$ (R = H, Me, Cl, Br, and NO_2); two acetate and two t-Busal-R′py^{2-} ligands are respectively located around the Ru_2 unit in a *trans* fashion, where the t-Busal-R′py^{2-} ligand acts as a tridentate ligand having both bridging and chelating characters to form the M–M bridging/axial-chelating mode. Their Ru–Ru bonded core with an electronic configuration of $\sigma^2\pi^4\delta^2(\pi^*\delta^*)^3$ is axial-capped by the di-t-butylphenolate groups of the t-Busal-R′py^{2-} ligands, and experiences multi-redox properties: a one-electron reduction to Ru_2^{4+} and two one-electron oxidations to Ru_2^{6+} followed by Ru_2^{7+}, in addition to t-Busal-R′py^{2-} ligand-centered redox. The strong electron-donating ability of the t-butyl groups compared with the other R-groups leads to negative shifts of the redox potentials according to the Hammett law.

Since the discovery of the Re–Re quadruple bond in $[Re_2Cl_8]^{2-}$,[1] paddlewheel-type metal–metal bonded compounds have been extensively studied over the past three decades,[2] principally from the viewpoint of the correlation between their core structures, including the metal–metal bond and the electronic structures on a set of M–M frontier orbitals, $\sigma\pi_2\delta\delta^*\pi^*_2\sigma^*$. The most fascinating feature of paddlewheel-type compounds is their multi-redox activity; the compounds undergo both oxidation and reduction on the dimetal center with a systematical change of the metal–metal bond length according to the electron arrangement on the frontier orbitals, but without a considerable structural change. Therefore, the electronic tuning of the metal–metal bonding core is an attractive theme. Indeed, several studies have shown that the tuning is realized by an electronic effect induced by remote substituents on the surrounding bridging ligands, in which the Hammett correlation has revealed the possibility of fine-tuning of the M–M based redox potentials.[3] The ligand-induced electronic effect could also be seen in dimetal compounds with specific bridging/chelating polydentate ligands. Such ligands are classified into three types in Chart 1: rigid N–N–N pyridyl type (I), N–N–O catecholate type (II), and N–N–O phenolate type (III). The common aspect in these bridging/chelating ligands is the existence of redox-active organic moieties corresponding to

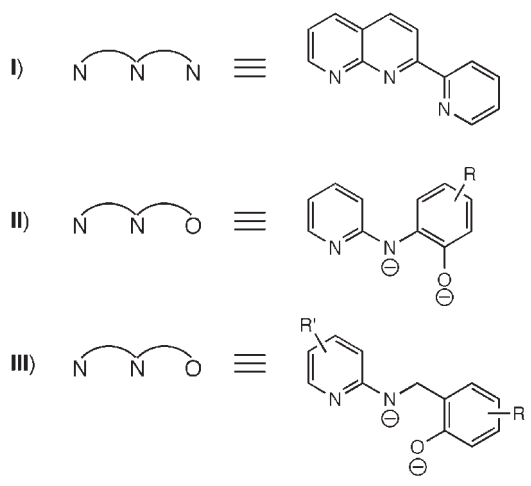

Chart 1.

Published on the web April 7, 2006; DOI: 10.1246/bcsj.79.612

1,8-naphthyridine in I,[4–6] 2-oxoanilino group in II,[7–9] and phenoxido group in III,[10,11] with which their dimetal compounds undergo not only metal-centered redox, but also ligand-centered redox. Moreover, some of them revealed d–π electron-conjugated redox behavior.

We focus on diruthenium compounds with the type **III** ligand, in which the phenolate component is redox-active, even in such dimetal compounds. The desired compounds have been synthesized by the ligand substitution reaction of tetrakis(acetato)diruthenium(II, III) with a family of redox-active tridentate ligands, *N*-(2-pyridyl)-2-oxido-R-benzylaminate (abbreviated as $Rsalpy^{2-}$), to produce a bis-substituted type of $[Ru_2(O_2CCH_3)_2(Rsalpy)_2]^{-}$[10] and a tris-substituted type of $[Ru_2(5\text{-}Clsalpy)_3]^{-}$.[11] Among them, bis-substituted compounds were first obtained by using 5-position-substituted ligands of type **III**, where 5-R corresponded to H, Me, Cl, Br, and NO_2 groups to form a series of $A[Ru_2(O_2CCH_3)_2(5\text{-}Rsalpy)_2]$ (A = counter cation).[10] In addition to metal-centered redox couplings (Ru_2^{5+}/Ru_2^{4+}, Ru_2^{6+}/Ru_2^{5+}, and Ru_2^{7+}/Ru_2^{6+}), oxidations of two 5-$Rsalpy^{2-}$ ligands in a compound were observed as an *irreversible* two-electron coupling at relatively high potentials of 0.70 (Me)–1.21 V (NO_2) (vs Ag/Ag^+) in accord with the Hammett law. The observation of only one coupling for the phenolate oxidations, unfortunately, suggests that the electronic interaction between the two phenoxido groups via the Ru_2 unit is almost negligible.

Based on this work, we prepared three new type **III** ligands, *N*-(2-pyridyl)-2-oxido-3,5-di-*tert*-butylbenzylaminate (*t*-$Busalpy^{2-}$), *N*-(4-methyl-2-pyridyl)-2-oxido-3,5-di-*tert*-butylbenzylaminate (*t*-Busal-4-$Mepy^{2-}$), and *N*-(5-methyl-2-pyridyl)-2-oxido-3,5-di-*tert*-butylbenzylaminate (*t*-Busal-5-$Mepy^{2-}$), and synthesized the corresponding diruthenium compounds: $[Na(18\text{-crown-}6)(thf)_2][Ru_2(O_2CCH_3)_2(t\text{-}Busalpy)_2]$ (**1**), $[K(18\text{-crown-}6)(thf)_2][Ru_2(O_2CCH_3)_2(t\text{-Busal-4-}Mepy)_2]$ (**2**), and $[K(18\text{-crown-}6)(thf)(H_2O)][K(18\text{-crown-}6)(thf)(MeO)][Ru_2(O_2CCH_3)_2(t\text{-Busal-5-}Mepy)_2]$ (**3**) (18-crown-6 = 1,4,7,-10,13,16-hexaoxocyclooctadecane; 18-crown-6-ether). It is well known that 3,5-di-*tert*-butylphenolate produces electrochemically a relatively persistent phenoxyl radical (reversible couple) in its metal complexes because of the strong electron-donating effect of the *tert*-butyl groups and the ortho and para substitutions of the parent phenolate, which provide resonance stabilization.[12] As expected, compounds **1** and **2** undergo the ligand-based redox as two separated quasi-*reversible* couples with $\Delta E_{1/2} = 96$ and 70 mV, respectively, in addition to the metal-centered redox, indicating a weak electronic interaction between the phenoxido groups via the Ru–Ru bond. By contrast, compound **3** undergoes phenolate dissociation on one of the two moieties during the metal-centered oxidation of Ru_2^{6+} to Ru_2^{7+}. We describe herein the syntheses, structures, and electrochemistry of these compounds.

Experimental

Materials and Reagents. Syntheses of diruthenium compounds were carried out under a dried nitrogen atmosphere. All chemicals used for the syntheses were of reagent grade. The diruthenium(II, III) compound $Ru_2(O_2CCH_3)_4Cl$ was synthesized according to a method in the literature.[13] All solvents used for the syntheses of the Ru_2 compounds and their electrochemical and spectroscopic studies were dried by refluxing over common drying agents and freshly distilled under a nitrogen atmosphere before use.

Preparation of Protonated Ligands, *t*-$BusalpyH_2$, *t*-Busal-4-$MepyH_2$, and *t*-Busal-5-$MepyH_2$. An ethanol solution of the corresponding Schiff-base compounds for the derivation of the reduced forms, *t*-$BusalpyH_2$, *t*-Busal-4-$MepyH_2$, and *t*-Busal-5-$MepyH_2$, was prepared by refluxing 3,5-di-*tert*-butylsalicylaldehyde (4.69 g, 20 mmol) and 2-aminopyridine (1.88 g, 20 mmol), 2-amino-4-picoline (2.16 g, 20 mmol), and 2-amino-5-picoline (2.16 g, 20 mmol), respectively, in ethanol (30 mL). Without isolating the Schiff-base compound, to the ethanol solution was slowly added solid $NaBH_4$ (756 mg, 20 mmol) at room temperature. During this time, the yellow suspension became a colorless solution. This solution was stirred overnight at room temperature. To the solution was slowly added water (100 mL) to form colorless block-shaped microcrystals of the ligands. The crude sample was recrystallized from an ethanol/water mixture. The crystalline sample was filtered, washed with water, and dried in vacuo over P_2O_5. Yield 1.9 g, 30% for *t*-$BusalpyH_2$; 2.7 g, 41% for *t*-Busal-4-$MepyH_2$; 3.6 g, 55% for *t*-Busal-5-$MepyH_2$. ***t*-$BusalpyH_2$**: Anal. Calcd for $C_{20}H_{28}N_2O$: C, 76.88; H, 9.03; N, 8.97%. Found: C, 76.82; H, 8.97; N, 8.88%. IR (KBr, cm^{-1}): 3433 (m, NH), 2959 (s, CH), 2588 (w, br, OH), 1618 (s), 1570 (w), 1510 (s), 1439 (m), 1236 (m), 1202 (w), 974 (w), 770 (m). ^1H NMR (500 MHz, $CDCl_3$): δ 11.69 (s, 1H, OH), 8.05 (m, 1H, C_{pyr}-H), 7.35 (m, 1H, C_{pyr}-H), 7.27, (d, 1H, $J = 2.5$ Hz, C_{ph}-H), 7.07 (d, 1H, $J = 2.5$ Hz, C_{ph}-H), 6.54 (t, 1H, $J = 6.1$ Hz, C_{pyr}-H), 6.42 (d, 1H, $J = 8.6$ Hz, C_{pyr}-H), 5.07 (t, 1H, $J = 6.2$ Hz, NH), 4.45 (2H, $J = 6.7$ Hz, CH_2), 1.43 (s, 9H, *t*-Bu), 1.30 (s, 9H, *t*-Bu). ***t*-Busal-4-$MepyH_2$**: Anal. Calcd for $C_{21}H_{30}N_2O$: C, 77.26; H, 9.26; N, 8.58%. Found: C, 76.85; H, 9.22; N, 8.35%. IR (KBr, cm^{-1}): 3315 (m, NH), 2951 (s, CH), 2588 (w, br, OH), 1632 (s), 1539 (m), 1441 (m), 1238 (m), 1186 (w), 980 (w), 789 (m). ^1H NMR (500 MHz, $CDCl_3$): δ 11.87 (s, 1H, OH), 7.92 (d, 1H, $J = 5.5$ Hz, C_{pyr}-H), 7.26 (d, 1H, $J = 1.6$ Hz, C_{ph}-H), 7.06 (d, 1H, $J = 2.5$ Hz, C_{ph}-H), 6.39 (dd, 1H, $J = 5.5$ Hz, 0.9 Hz, C_{pyr}-H), 6.22 (s, 1H, C_{pyr}-H), 4.98 (t, 1H, $J = 6.4$ Hz, NH), 4.43 (d, 2H, $J = 6.4$ Hz, CH_2), 2.18 (s, 3H, CH_3), 1.43 (s, 9H, *t*-Bu), 1.29 (s, 9H, *t*-Bu). ***t*-Busal-5-$MepyH_2$**: Anal. Calcd for $C_{21}H_{30}N_2O$: C, 77.26; H, 9.26; N, 8.58%. Found: C, 77.26; H, 9.34; N, 8.49%. IR (KBr, cm^{-1}): 3325 (s, NH), 2953 (s, CH), 2866 (m, CH), 2569 (m, br, OH), 1773 (w), 1632 (s), 1531 (s), 1481 (m), 1439 (s), 1360 (s), 1236 (s), 1161 (w), 881 (m), 822 (s). ^1H NMR (500 MHz, $CDCl_3$): δ 11.77 (s, 1H, OH), 7.88 (s, 1H, C_{pry}-H), 7.27 (d, 1H, $J = 2.5$ Hz, C_{ph}-H), 7.20 (m, 1H, C_{pyr}-H), 7.07 (d, 1H, $J = 2.5$ Hz, C_{ph}-H), 6.35 (d, 1H, $J = 8.3$ Hz, C_{pyr}-H), 4.94 (t, 1H, $J = 6.4$ Hz, NH), 4.42 (d, 2H, $J = 6.4$ Hz, CH_2), 2.15 (s, 3H, CH_3), 1.45 (s, 9H, *t*-Bu), 1.31 (s, 9H, *t*-Bu).

Preparation of Diruthenium Compounds 1–3. A mixture of *t*-$BusalpyH_2$ (187 mg, 0.6 mmol) for **1**, *t*-Busal-4-$MepyH_2$ (196 mg, 0.6 mmol) for **2**, or *t*-Busal-5-$MepyH_2$ (196 mg, 0.6 mmol) for **3** in 15 cm^3 of methanol containing NaOH (48 mg, 1.2 mmol) for **1**, or KOH (67 mg, 1.2 mmol) for **2** and **3** was added to solid $Ru_2(O_2CCH_3)_4Cl$ (142 mg, 0.3 mmol), and the brown suspension was stirred overnight at room temperature. During this time, the brown suspension became a dark-green solution with some precipitates. Then, the solution was filtered to remove any insoluble solids, and the filtrate was evaporated under reduced pressure. The green solid was dissolved again in 18 cm^3 of THF containing 18-crown-6-ether (317 mg, 1.2 mmol) and the obtained solution was stirred for 10 min at room temperature. The filtered solution was added into a narrow Schlenk tube for diffusion with 18 cm^3 of toluene to form rectangular green crystals. Other diffusion sol-

vents, such as *n*-hexane or diethyl ether, also resulted in the same products, but the purity of the sample was higher with toluene, although the yield seemed to be quite low. For **1**, yield 66 mg, 16%. Anal. Calcd for $C_{64}H_{98}N_4O_{14}NaRu_2$: C, 55.99; H, 7.20; N, 4.08%. Found: C, 55.41; H, 7.06; N, 3.91%. Mass spectral data (*m*/*z*): calculated for $C_{44}H_{58}N_4O_6Ru_2$ 941.3; MALDI-TOF found 941.6, 886.9, 825.7 ($[Ru_2(O_2CCH_3)_2(t\text{-Busalpy})_2]^-$, $[Ru_2(O_2CCH_3)(t\text{-Busalpy})_2]$, $[Ru_2(t\text{-Busalpy})_2]^+$). IR (KBr, cm^{-1}): 3413 (w, br), 2949 (m), 2903 (m), 1603 (m), 1468 (s), 1435 (s), 1352 (m), 1286 (m), 1109 (s), 837 (w). UV–vis (λ_{max}/nm ($\varepsilon/M^{-1}\,cm^{-1}$) in MeCN): 451 (5054), 592 (5573), 1046 (1304). For **2**·[K(18-crown-6)(CH_3O)(H_2O)], yield 90 mg, 19%. Anal. Calcd for $C_{79}H_{131}K_2N_4O_{22}Ru_2$: C, 53.62; H, 7.46; N, 3.17%. Found: C, 53.82; H, 7.17; N, 3.08%. Mass spectral data (*m*/*z*): calculated for $C_{46}H_{62}N_4O_6Ru_2$ 969.3; MALDI-TOF found 969.5, 914.9, 855.1 ($[Ru_2(O_2CCH_3)_2(t\text{-Busal-4-Mepy})_2]^-$, $[Ru_2(O_2CCH_3)(t\text{-Busal-4-Mepy})_2]$, $[Ru_2(t\text{-Busal-4-Mepy})_2]^+$). IR (KBr, cm^{-1}): 3385 (w, br), 2949 (s), 2901 (s), 1614 (s), 1462 (s), 1429 (s), 1352 (m), 1286 (m), 1109 (s), 964 (m), 827 (m). UV–vis (λ_{max}/nm ($\varepsilon/M^{-1}\,cm^{-1}$) in MeCN): 294 (27531), 442 (4198), 591 (5106), 1052 (565). For **3**, yield 50 mg, 9%. Anal. Calcd for $C_{79}H_{131}K_2N_4O_{22}Ru_2$: C, 53.62; H, 7.46; N, 3.17%. Found: C, 53.33; H, 7.28; N, 3.33%. Mass spectral data (*m*/*z*): calculated for $C_{46}H_{62}N_4O_6Ru_2$ 969.3; MALDI-TOF found 969.3, 910.9, 852.6 ($[Ru_2(O_2CCH_3)_2(t\text{-Busal-5-Mepy})_2]^-$, $[Ru_2(O_2CCH_3)(t\text{-Busal-5-Mepy})_2]$, $[Ru_2(t\text{-Busal-5-Mepy})_2]^+$). IR (KBr, cm^{-1}): 3454 (w), 2949 (m), 2899 (m), 1618 (m), 1578 (m), 1481 (m), 1437 (m), 1400 (m), 1352 (m), 1288 (m), 1109 (s), 962 (m), 843 (w). UV–vis (λ_{max}/nm ($\varepsilon/M^{-1}\,cm^{-1}$) in MeCN): 282 (32957), 465 (5792), 609 (5873), 1041 (1755).

Physical Measurements. Infrared spectra were measured on KBr disks with a Shimadzu FT-IR 8600 spectrophotometer. MALDI-TOF mass spectra were acquired on a Kratos Analytical KOMPACT PROBE. General magnetic susceptibility data for ground samples were measured over the temperature range of 1.9–300 K using an MPMS-XL SQUID susceptometer (Quantum Design, Inc.), where the applied magnetic fields were 1 T. Corrections were applied for diamagnetism using Pascal's constants[14] and for vinyl capsule wrapping samples. The UV–vis spectrum was measured in degassed acetonitrile in a septum-sealed cell using a Hitachi U-3500 spectrophotometer. Cyclic voltammograms (CVs) and differential pulse voltammograms (DPVs) were recorded in 1,2-dichloroethane (tetra-*n*-butylammonium hexafluorophosphate [*n*-$Bu_4N(PF_6)$] = 0.2 M as supporting electrolyte) under a nitrogen atmosphere with the use of an ALS/CHI Instruments Electrochemical Analyzer (model CHI 600A). At the beginning of measurement of the compounds, the CVs of 1,2-dichloroethane with only supporting electrolyte were measured. To this solution were added the compounds ([Compound] = 2×10^{-3} M) and measured with one unit of a carbon working electrode, a Pt counter electrode, and a $Ag/AgNO_3$ reference electrode. Finally, CV potentials were justified by using the ferrocene/ferrocenium couple as an internal reference ($Fc/Fc^+ = 0.194$ V ($\Delta E = 123$ mV) in 1,2-dichloroethane vs $Ag/AgNO_3$).

X-ray Crystallographic Analyses. Measurements were made on a Rigaku CCD diffractometer for **1** and on a Rigaku Imaging Plate diffractometer for **2** and **3** with graphite monochromated Mo Kα radiation ($\lambda = 0.71069$ Å). The data were collected at -170 ± 1 °C for all compounds. An empirical absorption correction based on azimuthal scans of several reflections was applied. The structures were solved by direct methods (SIR92)[15] and expanded using Fourier techniques.[16] The non-hydrogen atoms were refined anisotropically, whereas the hydrogen atoms were refined isotropically. For full-matrix least-squares refinements based on the $I > 2.00\sigma(I)$ reflections and the observed reflections, the unweighted and weighted agreement factors of $R1 = \Sigma||F_o| - |F_c||/\Sigma|F_o|$ ($I > 2.00\sigma(I)$), $R2 = \Sigma(F_o^2 - F_c^2)/\Sigma F_o^2$ (all data), and $R_w = [\Sigma w(F_o^2 - F_c^2)^2/\Sigma w(F_o)^2]^{1/2}$ (all data) were used. The weighting scheme was based on counting statistics. All calculations were performed using the teXsan crystallographic software package of Molecular Structure Corporation.[17] The crystal data and details of the structure determinations for **1**–**3** are summarized in Table 1. Crystallographic data (excluding structure factors) for the structures of **1**–**3** have been deposited at the Cambridge Data Centre as supplementary publication Nos. CCDC-286435 for **1**, CCDC-286433 for **2**, and CCDC-286434 for **3**. Copies of the data can be obtained free of charge via http://www.ccdc.cam.ac.uk/conts/retrieving.html, or from the Cambridge Crystallographic Data Centre, 12, Union Road, Cambridge, CB2 1EZ, UK (fax: +44 1223 336033; e-mail: deposit@ccdc.cam.ac.uk).

Results and Discussion

Syntheses and General Properties. The protonated tridentate ligands that correspond to the amine species, *t*-Busal-R′pyH_2, were obtained by reducing the corresponding Schiff-base compounds with $NaBH_4$ in methanol. Completion of the reduction was easily confirmed by a change in color of the solution from light yellow to colorless. Crystallization in a methanol/water mixture produced well-shaped crystals of *t*-Busal-R′pyH_2 (R′ = H, 4-Me, and 5-Me). In the IR spectra, the vibration of C=N (imine; ν = ca. 1600 cm^{-1}) in Schiff-base compounds was no longer detected in the reduced species. In the ^{1}H NMR spectra, a triplet corresponding to amino proton (–NH) was newly observed in the reduced species at 5.07 ppm for *t*-BusalpyH$_2$, 4.98 ppm for *t*-Busal-4-MepyH$_2$, and 4.94 ppm for *t*-Busal-5-MepyH$_2$.

Bis-substitution of the acetato ligands of the paddlewheel-type diruthenium compound $Ru_2(O_2CCH_3)_4Cl$ with *t*-Busal-R′pyH_2 was accomplished under a methanolic condition in a 1:2 molar ratio of $Ru_2(O_2CCH_3)_4Cl$:*t*-Busal-R′pyH_2 in the presence of NaOH or KOH as the deprotonation reagent. The addition of 18-crown-6-ether to form the Na^+- or K^+-crown-ether cationic complex led to the successful crystallization of **1**–**3**. Thus, compounds **1**–**3** are composed of the Na^+- or K^+-crown-ether cation and diruthenium anionic species, as shown in Scheme 1. The stability of the anionic components, $[Ru_2(O_2CCH_3)_2(t\text{-Busal-R′py})_2]^-$, was first checked by MALDI-TOF mass spectroscopy in an experimental nujol medium (see Experimental). The main signal assigned to $[Ru_2(O_2CCH_3)_2(t\text{-Busal-R′py})_2]^-$ was detected at 941.6 (*m*/*z*, 941.3), 969.5 (*m*/*z*, 969.3), and 969.3 (*m*/*z*, 969.3), respectively, for **1**–**3**, with two characteristic minor signals attributed to the acetate-eliminated species of $[Ru_2(O_2CCH_3)(t\text{-Busal-R′py})_2]$ and $[Ru_2(t\text{-Busal-R′py})_2]^+$, proving the formation of the present bis-substituted compounds. Because a confirmation of the magnetic data is useful for determining the electronic state of a diruthenium unit, the magnetic susceptibilities of **1**–**3** were measured in the temperature range of 1.9–300 K. For all compounds, the χT products at 300 K were found in the range of 1.88–1.97 $cm^3\,K\,mol^{-1}$. Then, upon cooling, they gradually decreased to finally reach minimum values (0.39–1.06 $cm^3\,K\,mol^{-1}$). The room temperature χT values are very sim-

Table 1. Crystallographic Data of **1–3**

	1	**2**·2THF	**3**
Empirical formula	$C_{64}H_{98}N_4O_{14}NaRu_2$	$C_{74}H_{118}KN_4O_{16}Ru_2$	$C_{79}H_{131}K_2N_4O_{22}Ru_2$
Fw/g mol^{-1}	1372.830	1561.207	1769.459
Space group	$C2/c$ (#15)	$P\bar{1}$ (#2)	$P\bar{1}$ (#2)
T/°C	−150(1)	−170(1)	−170(1)
λ/Å	0.7107	0.7107	0.7107
a/Å	21.6776(6)	11.017(2)	9.6966(5)
b/Å	16.5661(4)	13.406(3)	13.1709(7)
c/Å	20.9809(7)	15.162(3)	18.212(1)
α/deg	90	115.019(9)	77.362(2)
β/deg	103.6283(4)	92.691(8)	77.797(3)
γ/deg	90	104.948(8)	85.157(2)
V/Å^3	7322.4(4)	1929.2(6)	2216.5(2)
Z	4	1	1
D_{calcd}/g cm^{-3}	1.245	1.344	1.325
μ(Mo Kα)/cm^{-1}	4.77	5.11	5.04
Unique reflns.	8381 ($I > 2.00\sigma(I)$)	8332 ($I > 2.00\sigma(I)$)	8984 ($I > 2.00\sigma(I)$)
No. variables	382	439	505
GOF	0.999	1.361	1.883
$R1$[a)]	0.0758 ($I > 2.00\sigma(I)$)	0.0480 ($I > 2.00\sigma(I)$)	0.0750 ($I > 2.00\sigma(I)$)
$wR2$	0.2301 (all data)	0.1445 (all data)	0.2411 (all data)

a) $R1 = \Sigma||F_o| - |F_c||/\Sigma|F_o|$. b) $wR2 = [\Sigma w(F_o^2 - F_c^2)^2/\Sigma w(F_o^2)^2]^{1/2}$. c) $w = 1/[\sigma^2 F_o^2 + (p(\max(F_o^2, 0) + 2F_c^2)/3)^2]$ for **1**, where $p = 0.11300$ for **1**, 0.08900 for **2**, $w = 1/[\sigma^2 F_o^2 + (0.1000P)^2]$, where $P = (F_o^2 + 2F_c^2)/3$ for **3**.

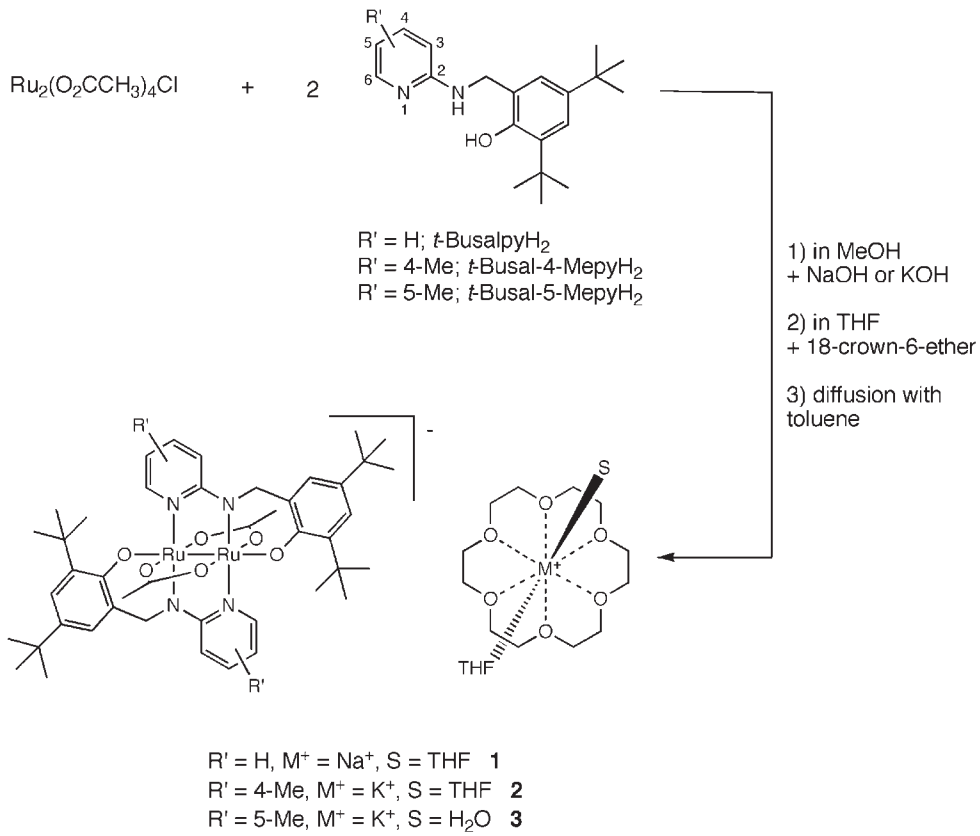

Scheme 1.

ilar to those observed in this class of diruthenium compounds; for example, 2.00–2.31 cm^3 K mol^{-1} for $[Ru_2(O_2CR)_4]^+$ and $Ru_2(O_2CR)_4Cl$, possessing an $S = 3/2$ spin ground state.[18–27] The decrease of the χT product should be principally due to the contribution of zero-field splitting (ZFS) arising from the $^4B_{2u}$ electronic ground state.[28,29] To take into account the decrease of χT, best-fitting using the $S = 3/2$ paramagnetic Van Vleck approximation with the ZFS contribution (D)[30] and the inter-molecular interaction (zJ)[31] was performed, and the best agreement between the model and the experiment

was obtained with the following parameters: $g = 2.05$, $D = 57.3\,cm^{-1}$, $zJ = -0.06\,cm^{-1}$ ($R = 0.9981$) for **1**; $g = 2.02$, $D = 64.0\,cm^{-1}$, $zJ = -0.06\,cm^{-1}$ ($R = 0.9990$) for **2**; $g = 2.08$, $D = 53.5\,cm^{-1}$, $zJ = -0.88\,cm^{-1}$ ($R = 0.9990$) for **3** ($R = 1 - \Sigma\{(\chi T_{calc} - \chi T_{obs})/\Sigma(\chi T_{obs})\}^2$). All of the above parameters are in good agreement with previously reported values for paddlewheel-type diruthenium compounds ($D \approx 40$–$90\,cm^{-1}$).[18–27,29] Consequently, the electronic configuration of **1**–**3** could be $\sigma^2\pi^4\delta^2(\pi^*\delta^*)^3$.

The UV–vis spectra of **1**–**3** were recorded in MeCN under N_2 (Fig. 1 and Table 2). All compounds exhibited relatively strong bands in the UV–vis region at around 300 nm (sh), 380 nm (sh), 450 nm ($\varepsilon \approx 5000$–$6000\,M^{-1}\,cm^{-1}$), and 600 nm ($\varepsilon \approx 6000\,M^{-1}\,cm^{-1}$), the last one of which is understandable because of the intense green color of **1**–**3**. In addition, a weak band at around 1050 nm ($\varepsilon \approx 1000$–$1800\,M^{-1}\,cm^{-1}$) was also observed. The overall spectral feature is very similar to that of the family of $A[Ru_2(O_2CCH_3)_2(5\text{-Rsalpy})_2]$.[10]

Structures of 1–3. *t*-Busal-R′py^{2-} acts as a dianionic tridentate ligand containing aminopyridyl and phenolate moieties that are connected to each other by a methylene group, where the former could attach to the diruthenium unit and the latter could flexibly coordinate to the axial positions of the Ru–Ru bond. All solid-state structures of the anionic components were thus confirmed to have a similar geometrical form. ORTEP drawings of the diruthenium anionic components of **1**–**3** are depicted in Fig. 2. Selected bond distances and angles around the diruthenium unit are summarized in Table 3. In this type of compound, the equatorial ligands are located around a diruthenium unit in *trans*-fashion; however, this is rare and most cases show localization in *cis*-fashion.[6,7,9] The Ru–Ru bond distance gives a typical value of 2.301(1) Å for **1**, 2.3114(4) Å for **2**, and 2.3091(4) Å for **3**, which seems to be similar to those of analogues $A[Ru_2(O_2CCH_3)_2(5\text{-Rsalpy})_2]$ (R = H, Me, Cl, Br, and NO_2) (2.28–2.30 Å), and follows the trend 5-NO_2 < 5-Cl, 5-Br < H ≈ 5-Me ≈ **1** < **2**, **3**, due to the electron-donating ability of remote substituents. The typical value of the Ru–

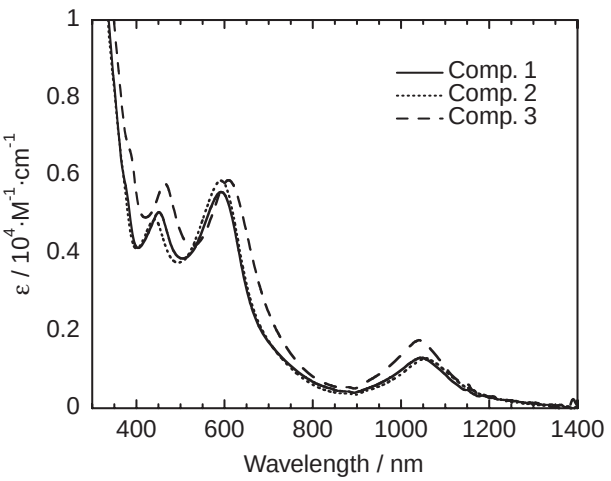

Fig. 1. UV–vis–NIR spectra of **1**–**3** in MeCN.

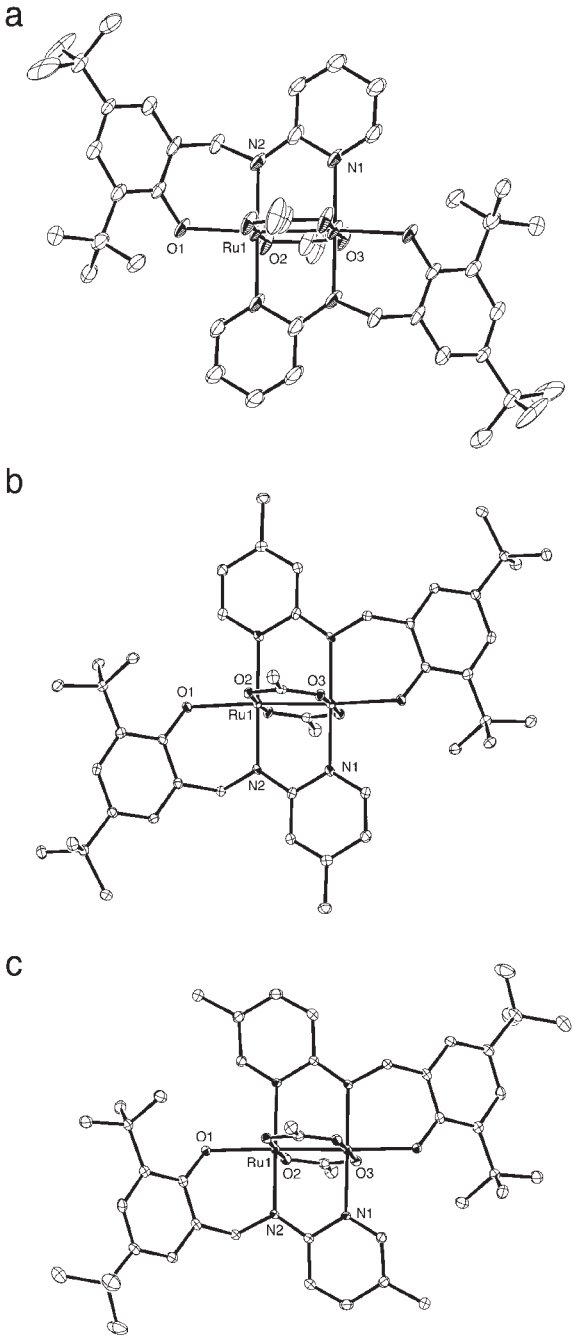

Fig. 2. Structure drawings of an asymmetrical anionic unit of **1** (a), **2** (b), and **3** (c).

Table 2. UV–Vis–NIR Spectral Data of **1**–**3** in MeCN under N_2

	λ_{max}/nm ($\varepsilon/10^3\,M^{-1}\,cm^{-1}$)				
Compd	Band I	Band II	Band III	Band IV	Band V
1	300 (sh)	374 (sh)	451 (5.0)	592 (5.6)	1046 (1.3)
2	290 (sh)	370 (sh)	441 (4.9)	591 (5.9)	1052 (1.3)
3	282 (sh)	380 (sh)	465 (5.8)	609 (5.9)	1041 (1.8)

Table 3. Relevant Bond Distances (Å) and Angles (deg) of **1–3** with Estimated Standard Deviations in Parentheses

	1	**2**·2THF	**3**
		Distances/Å	
Ru(1)–Ru(1)*[a)]	2.301(1)	2.3114(4)	2.3091(4)
Ru(1)–O(1)	2.178(4)	2.194(2)	2.193(3)
Ru(1)–O(2)	2.035(5)	2.056(2)	2.052(2)
Ru(1)–O(3)*	2.065(5)	2.037(2)	2.074(2)
Ru(1)–N(1)*	2.056(6)	2.075(2)	2.070(3)
Ru(1)–N(2)	2.026(7)	2.034(2)	2.037(3)
		Angles/deg	
Ru(1)*–Ru(1)–O(1)	172.5(1)	174.17(5)	172.83(7)
Ru(1)*–Ru(1)–O(2)	91.6(1)	87.22(6)	90.59(8)
Ru(1)*–Ru(1)–O(3)*	87.0(1)	91.16(6)	87.74(8)
Ru(1)*–Ru(1)–N(1)*	90.4(2)	91.09(7)	90.88(9)
Ru(1)*–Ru(1)–N(2)	89.3(2)	88.77(7)	89.15(9)
O(1)–Ru(1)–O(2)	95.3(2)	88.60(8)	95.9(1)
O(1)–Ru(1)–O(3)*	86.2(2)	93.10(8)	85.82(10)
O(1)–Ru(1)–N(1)*	92.8(2)	92.98(9)	92.2(1)
O(1)–Ru(1)–N(2)	87.9(2)	87.49(9)	88.2(1)
O(2)–Ru(1)–O(3)*	178.1(2)	178.02(7)	178.2(1)
O(2)–Ru(1)–N(1)*	88.4(2)	89.95(8)	90.4(1)
O(2)–Ru(1)–N(2)	87.8(2)	94.33(9)	86.3(1)
O(3)*–Ru(1)–N(1)*	90.3(2)	88.93(9)	88.98(10)
O(3)*–Ru(1)–N(2)	93.5(2)	86.78(9)	94.3(1)
N(1)*–Ru(1)–N(2)	176.2(2)	175.70(9)	176.7(1)

a) Symmetry operations (*): $-x+1/2$, $-y+1/2$, $-z$ for **1**; $-x$, $-y$, $-z+1$ for **2**; $-x+2$, $-y$, $-z$ for **3**.

Ru bond distance is one proof of the Ru_2^{5+} center with the electronic configuration of $\sigma^2\pi^4\delta^2(\pi^*\delta^*)^3$.[18–27] As mentioned above, the aminopyridyl moiety of the *t*-Busal-R′py^{2-} ligand bridges the diruthenium unit with bond distances of $(Ru–N_{pyridine})_{av} = 2.067$ Å and $(Ru–N_{aminato})_{av} = 2.032$ Å, in which the latter is slightly shorter than the former. The bond distances between Ru and carboxylate oxygen are found in the range of 2.035–2.074 Å. Two phenolate moieties as pendant ligands cap the axial positions of the Ru–Ru bond with distances and angles of Ru(1)–O(1) = 2.178(4) Å and O(1)–Ru(1)–Ru(1)* = 172.5(1)° for **1**, Ru(1)–O(1) = 2.194(2) Å and O(1)–Ru(1)–Ru(1)* = 174.17(5)° for **2**, and Ru(1)–O(1) = 2.193(3) Å and O(1)–Ru(1)–Ru(1)* = 172.83(7)° for **3**. The Ru–O distance is slightly shorter than that in A[$Ru_2(O_2CCH_3)_2$(5-Rsalpy)$_2$] (R = H, Me, Cl, Br, and NO_2) with the trend of 5-NO_2 ≈ H > 5-Cl, 5-Br > 5-Me > **2**, **3** > **1**; the remote substituent effect can also be seen here.

Electrochemistry of 1–3. The electronic behavior of **1–3** was confirmed by cyclic voltammetry (CV) and differential pulse voltammetry (DPV) in 1,2-dichloroethane containing *n*-$Bu_4N(PF_6)$ as the supporting electrolyte (vs $Ag/AgNO_3$). Both kinds of voltammograms for **1–3** are shown in Fig. 3, and the obtained electrochemical data are summarized in Table 4 together with those of the family of A[$Ru_2(O_2CCH_3)_2$(5-Rsalpy)$_2$] (R = H, Cl, Br, Me, and NO_2). All compounds revealed rich redox chemistry and basically identical redox processes that included principally one reduction and four oxidations. Some additional redox waves representative of structure-modified species were noted in **3** during measurements (vide infra). The one-electron reduction was observed around

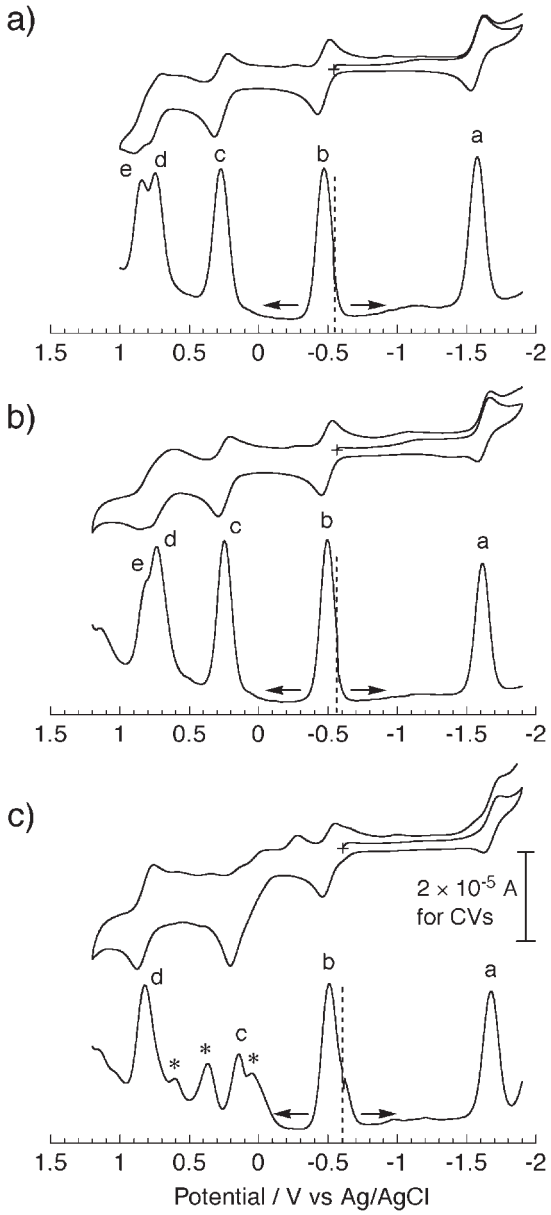

Fig. 3. Cyclic and differential pulse voltammograms of **1–3** in 1,2-dichloroethane containing 0.2 M TBA(PF_6) under N_2. The arrow in the DPV displays the sweep direction from the rest potential.

−1.6 V as a reversible wave ($I_a/I_c \approx 1$, $\Delta E_p \approx 90$ mV), and was assigned to a metal-based 1e$^-$ reduction of Ru_2^{5+}/Ru_2^{4+}. For the oxidation processes, the first and second couples were assigned to the metal-based ones, Ru_2^{6+}/Ru_2^{5+} and Ru_2^{7+}/Ru_2^{6+}, respectively. These values were shifted more negatively than the corresponding values for [$Ru_2(O_2CCH_3)_2$-(5-Rsalpy)$_2$]$^-$. Indeed, the one-electron oxidation of **1** to form the Ru_2^{6+} species occured at −0.469 V, which was more negative than −0.371 V of [$Ru_2(O_2CCH_3)_2$(5-Mesalpy)$_2$]$^-$, −0.326 V of [$Ru_2(O_2CCH_3)_2$(salpy)$_2$]$^-$, or −0.238 V of [Ru_2-$(O_2CCH_3)_2$(5-Clsalpy)$_2$]$^-$. The redox shifts should be due to the ligand-substituent effect on the R-group in the [Ru_2-$(O_2CCH_3)_2$(R-salpy)$_2$]$^-$ family, where there could be a strong electron-donating effect when R = 3,5-di-*t*-butyl group. There-

Table 4. Electrochemical Data of **1**–**3** Measured in 1,2-Dichloroethane Containing 0.2 M TBA(PF_6) under N_2 (V vs Ag/$AgNO_3$)[a)]

Compd	A Ru_2^{5+}/Ru_2^{4+}	B Ru_2^{6+}/Ru_2^{5+}	C Ru_2^{7+}/Ru_2^{6+}	D L/L$^-$	E L/L$^-$	$\Delta E_{1/2}$(E–D) mV[d)]	K_c[e)]
1	−1.576[b)]	−0.469[b)]	0.274[b)]	0.806[f)]	0.902[f)]	96	42
	(−1.577)[c)]	(−0.471)[c)]	(0.272)[c)]	(0.747)[c)]	(0.843)[c)]		
2	−1.613[b)]	−0.491[b)]	0.248[b)]	0.790[f)]	0.858[f)]	70	15
	(−1.613)[c)]	(−0.494)[c)]	(0.247)[c)]	(0.736)[c)]	(0.806)[c)]		
3	−1.682[b)]	−0.506[b)]	0.205[f)]	0.818	—	—	—
	(−1.676)[c)]	(−0.509)[c)]	(0.144)[c)]	(0.818)[c)]			
H	−1.511[b)]	−0.326[b)]	0.281[b)]	0.867[b)]	—	—	—
	(−1.490)[c)]	(−0.316)[c)]	(0.252)[c)]	(0.810)[c)]			
5-Me[g)]	−1.504[b)]	−0.371[b)]	0.259[b)]	0.704[b)]	0.864[f)]	135	192
	(−1.506)[c)]	(−0.381)[c)]	(0.220)[c)]	(0.675)[c)]	(0.810)[c)]		
5-Cl[g)]	−1.446[b)]	−0.238[b)]	0.355[b)]	0.982[b)]	—	—	—
	(−1.440)[c)]	(−0.254)[c)]	(0.312)[c)]	(0.886)[c)]			
5-Br[g)]	−1.427[b)]	−0.227[b)]	0.361[b)]	0.977[b)]	—	—	—
	(−1.417)[c)]	(−0.218)[c)]	(0.330)[c)]	(0.908)[c)]			
5-NO_2[g)]	−1.282[b)]	−0.029[b)]	0.585[b)]	1.205[b)]	—	—	—
	(−1.274)[c)]	(−0.029)[c)]	(0.394)[c)]	(1.082)[c)]			

a) The ferrocene/ferrocenium couple, $Fc/Fc^+ = 0.194$ V ($I_c/I_a \approx 1$, $\Delta E_p = 123$ mV), was observed at the same condition described in the Experimental Section in the text. b) Half-wave potentials ($E_{1/2}$'s) from cyclic voltammograms. The couples of A, B, and C were estimated because of their reversibility ($I_c/I_a \approx 1$, $\Delta E_p \approx 100$ mV at a scan rate of 0.03 V s^{-1}). c) Peak potentials from differential pulse voltammograms (scan rate, 8 mV s^{-1}; pulse width, 60 ms; pulse period, 120 ms). d) $\Delta E_{1/2}{}^{1-2}$ were calculated by using the DPV peak half-height method of Richardson and Taube.[32] e) Comproportionation constant (K_c), calculated by using the equation of $K_c = \exp(\Delta E_{1/2}/25.69)$ (at 298 K).[32] f) Anode peaks because of their irreversibility. g) The electrochemical data have been measured at an acetonitrile solution quoted in Ref. 10b.

fore, the respective redox potentials were plotted as a function of the summation of the Hammett constants (σ), and are shown in Fig. 4a. The respective potentials exhibited a linear relationship.

The third and fourth redox couples corresponded to the 1e$^-$ oxidation of individual *t*-Busal-R′py^{2-} ligands. Interestingly, when R = H, 5-Cl, 5-Br, and 5-NO_2 in R-salpy, the redox for the corresponding ligand was observed as one couple of two one-electron oxidations, and when R = 5-Me, each oxidation was detected separately with a peak-to-peak separation of $\Delta_p = 135$ mV on DPV (CV did not clearly show the peak separation).[10b] The finding suggests that the electron-donating ability of the methyl and *t*-butyl substituted groups affected the HOMO/LUMO energy levels of not only the ligand, but also the diruthenium center. From the DPV data, the peak-to-peak separations between the third and fourth peaks of **1** and **2** were 100 and 76 mV, respectively. A more accurate calculation of $\Delta E_{1/2}{}^{1ox-2ox}$ was accomplished using the DPV peak half-height method of Richardson and Taube to give 96 mV for **1** and 70 mV for **2**.[32] Therefore, these values lead to a comproportionation constant, K_c, of 42 for **1** and 15 for **2**, for the redox reaction $K_c = \exp(\Delta E_{1/2}/25.69)$ at 298 K.[33] This constant could be related to the degree of electronic communication between ligands, probably via the Ru_2^{7+} unit. However, the calculated values are basically small, so that the degree of electronic communication between ligands seems to be low, being Class I in the Robin–Day classification for electron delocalization.[33] The K_c values are slightly different among **1**, **2**, and the R = 5-Me species. We cannot exclude the possibility of estimation errors because of the indefinite peak separation, as shown in Fig. 3. However, their values may include, even if minimally, the electronic effect of the methyl group attached to the pyridyl moiety of the ligands; i.e., the R′-substituent effect on the 4-position (*trans* vs pyridine N) in **2**, and the 5-position (*trans* vs pyridylamine) in **3**. Considering the Hammett substituent constants (σ) of H, *p*-Me, and *m*-Me for **1**–**3**, respectively, the respective redox potentials on the Ru_2 center and the ligand (a to e in Fig. 3) have a linear relationship as a function of 2σ, where 2 is the number of substituents per unit (Fig. 4b). Unfortunately, the difference in the comproportionation constants among **1**, **2**, and the R = 5-Me species could not be well understood from the relationship of substituent donation.

As mentioned above, repeated redox cycling in the measuring window led to the appearance of new waves around 0 and 0.5 V, especially as shown in Fig. 3c for **3** (* marked). These waves were not formed when the measurements were repeated at a range lower than −0.3 V that includes redox reactions of Ru_2^{5+}/Ru_2^{4+} and Ru_2^{6+}/Ru_2^{5+}. Therefore, during oxidation to Ru_2^{7+} and/or redox reactions on the ligands, some of the molecules would be modified to form axial-free species. Nevertheless, since a redox on the *t*-Busal-5-Mepy^{2-} ligand is observed as a reversible wave, even at 0.8 V, the mono-capped species, as shown in Scheme 2, is plausible. Although the non-capped species, of which both phenoxido groups are coordination-free, could be considered, the following results dismiss such an idea concerning the presence of the non-capped species: (i) the half-height width of DPV peak at 0.8 V in **3** is approximately half of the corresponding values in **1** and **2**, indicating one-electron oxidation per the mono-capped spe-

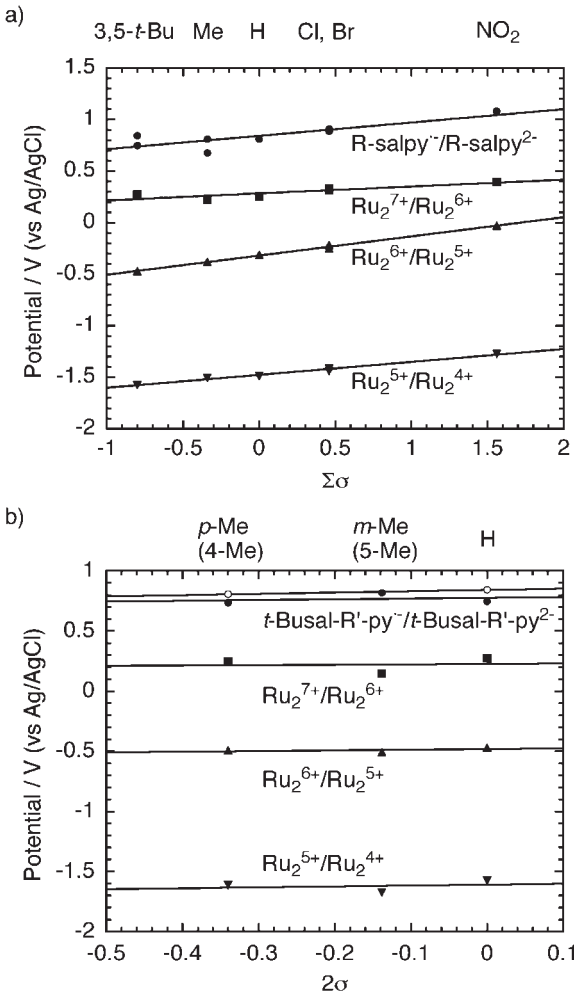

Fig. 4. Hammett plots of redox potentials (vs $Ag/AgNO_3$) on $[Ru_2(O_2CCH_3)_2(5\text{-Rsalpy})_2]^-$ (R = H, Me, Cl, Br, and NO_2)[10] and **1** (a), where $\Sigma\sigma$ is the summation of Hammett constants for all R-substituents, and on **1**–**3** (b), where σ is the Hammett constant for Me group (R′) on *t*-Busal-R′py and 2 is the number of substituents. For the referred potentials, the peak potentials in differential pulse voltammograms are used.

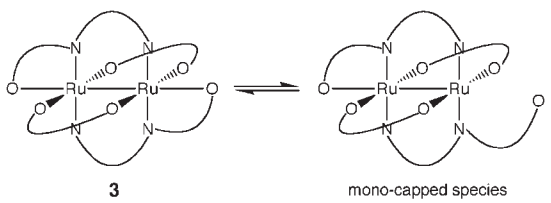

Scheme 2.

cies, (ii) the oxidation coupling on free-phanolate group does not appear at 0.8 V, rather showing a lower potential as a non-reversible wave. It is however uncertain why only **3** shows such a modification.

Summary

Three new tridentate bridging/chelating ligands, *N*-(2-pyridyl)-2-oxido-3,5-di-*tert*-butylbenzylaminate (*t*-Busalpy^{2-}), *N*-(4-methyl-2-pyridyl)-2-oxido-3,5-di-*tert*-butylbenzylaminate (*t*-Busal-4-Mepy^{2-}), and *N*-(5-methyl-2-pyridyl)-2-oxido-3,5-di-*tert*-butylbenzylaminate (*t*-Busal-5-Mepy^{2-}), have been prepared, and the corresponding diruthenium compounds, $[Na(18\text{-crown-6})(thf)_2][Ru_2(O_2CCH_3)_2(t\text{-Busalpy})_2]$ (**1**), $[K(18\text{-crown-6})(thf)_2][Ru_2(O_2CCH_3)_2(t\text{-Busal-4-Mepy})_2]$ (**2**), and $[K(18\text{-crown-6})(thf)(H_2O)][K(18\text{-crown-6})(thf)(MeO)][Ru_2(O_2CCH_3)_2(t\text{-Busal-5-Mepy})_2]$ (**3**), have been synthesized and isolated, thanks to the large counter cation of the Na- or K-18-crown-6-ether complex that stabilizes the crystallinity of the materials. Compounds **1**–**3** have a Ru–Ru bonded core with an electronic configuration of $\sigma^2\pi^4\delta^2(\pi^*\delta^*)^3$, which is axial-capped by the di-*t*-butylphenoxido groups of the *t*-Busal-R′py^{2-} ligands. The electrochemistry of these compounds reveals multi-redox properties on both the Ru_2-center and the *t*-Busal-R′py^{2-} ligands. Compared with the previously reported family of $[Ru_2(O_2CCH_3)_2(5\text{-Rsalpy})_2]^-$ (R = H, Me, Cl, Br, and NO_2), the strong electron-donating ability of the *t*-butyl groups compared with the other R-groups leads to significant shifts of the redox potentials according to the Hammett law. With the establishment of electronic communication between phenoxido groups via the Ru–Ru bond as our objective, we observed a sign of electronic communication in **1** and **2**, as well as the R = Me compound reported previously, albeit small. In addition, the introduction of a methyl group to the pyridine of the ligands (for **2** and **3**) does not provide any meaningful substituent effects for electronic communication. A further ligand modification and exchange of metal ion to control the HOMO/LUMO energy levels between the metal center and the ligand are in progress.

This work was partially supported by CREST project, the Japan Science and Technology Agency (JST) and a Grant-in-Aid for Scientific Research from the Ministry of Education, Culture, Sports, Science and Technology, Japan.

References

1 a) F. A. Cotton, C. B. Harris, *Inorg. Chem.* **1965**, *4*, 330. b) F. A. Cotton, *Inorg. Chem.* **1965**, *4*, 334.

2 F. A. Cotton, R. A. Walton, *Multiple Bonds between Metal Atoms*, Oxford University Press, Oxford, **1993**.

3 a) C. Lin, J. D. Protasiewicz, E. T. Smith, T. Ren, *J. Chem. Soc., Chem. Commun.* **1995**, 2257. b) C. Lin, J. D. Protasiewicz, E. T. Smith, T. Ren, *Inorg. Chem.* **1996**, *35*, 6422. c) C. Lin, J. D. Protasiewicz, T. Ren, *Inorg. Chem.* **1996**, *35*, 7455. d) C. Lin, T. Ren, E. J. Valente, J. D. Zubkowski, E. T. Smith, *Chem. Lett.* **1997**, 753. e) K. M. Carlson-Day, J. L. Eglin, C. Lin, L. T. Smith, R. J. Staples, D. O. Wipf, *Polyhedron* **1999**, *18*, 817. f) N. G. Connelly, P. R. G. Davis, E. E. Harry, P. Klangsinsirikul, M. Venter, *J. Chem. Soc., Dalton Trans.* **2000**, 2273. g) K. M. Kadish, L. Wang, A. Thuriere, E. V. Caemelbecke, J. L. Bear, *Inorg. Chem.* **2003**, *42*, 834.

4 W. R. Tikkanen, E. Binamira-Soriaga, W. C. Kaska, P. Ford, *Inorg. Chem.* **1984**, *23*, 141.

5 A. T. Baker, W. R. Tikkanen, W. C. Kaska, P. Ford, *Inorg. Chem.* **1984**, *23*, 3254.

6 a) C. S. Campos-Fernández, X. Ouyang, K. R. Dunbar, *Inorg. Chem.* **2000**, *39*, 2432. b) C. S. Campos-Fernández, L. M. Thomson, J. R. Galán-Mascarós, X. Ouyang, K. R. Dunbar, *Inorg. Chem.* **2002**, *41*, 1523.

7 L. Bear, Y. Li, B. Han, E. V. Caemelbecke, K. M. Kadish,

Inorg. Chem. **2001**, *40*, 182.
8 L. Bear, Y. Li, B. Han, E. V. Caemelbecke, K. M. Kadish, *Inorg. Chem.* **1996**, *35*, 3053.
9 T. Ren, V. DeSilva, G. Zou, C. Lin, L. M. Daniels, C. F. Campana, J. C. Alvarez, *Inorg. Chem. Commun.* **1999**, *2*, 301.
10 a) H. Miyasaka, C. Kachi-Terajima, T. Ishii, M. Yamashita, *J. Chem. Soc., Dalton Trans.* **2001**, 1929. b) H. Miyasaka, T. Izawa, K. Sugiura, M. Yamashita, *Inorg. Chem.* **2003**, *42*, 7683.
11 H. Miyasaka, K. Sugiura, M. Yamashita, *Inorg. Chem. Commun.* **2003**, *6*, 1078.
12 P. Chaudhuri, K. Wieghardt, *Prog. Inorg. Chem.* **2001**, *50*, 151.
13 R. W. Mitchell, A. Spencer, G. Wilkinson, *J. Chem. Soc., Dalton Trans.* **1973**, 846.
14 E. A. Boudreaux, L. N. Mulay, *Theory and Applications of Molecular Paramagnetism*, John Wiley & Sons, New York, **1976**, pp. 491–495.
15 A. Altomare, M. C. Burla, M. Camalli, M. Cascarano, C. Giacovazzo, A. Guagliardi, G. Polidori, *J. Appl. Crystallogr.* **1994**, *27*, 435.
16 P. T. Beurskens, G. Admiraal, G. Beurskens, W. P. Bosman, R. de Gelder, R. Israel, J. M. M. Smits, *The DIRDIF Program System*, Technical Report of the Crystallography Laboratory, University of Nijmegen, The Netherlands, **1994**.
17 *Crystal Structure Analysis Package*, Molecular Structure Corporation, The Woodlands, TX, **1985** and **1992**.
18 M. A. S. Aquino, *Coord. Chem. Rev.* **1998**, *170*, 141.
19 R. Jiménez-Aparicio, F. A. Urbanos, J. M. Arrieta, *Inorg. Chem.* **2001**, *40*, 613.
20 E. J. Beck, K. D. Drysdale, L. K. Thompson, L. Li, C. A. Murphy, M. A. S. Aquino, *Inorg. Chim. Acta* **1998**, *279*, 121.
21 M. C. Barral, R. Jiménez-Aparicio, D. Pérez-Quintanilla, J. L. Priego, E. C. Royer, M. R. Torres, F. A. Urbanos, *Inorg. Chem.* **2000**, *39*, 65.
22 F. D. Cukiernik, A.-M. Giroud-Godquin, P. Maldivi, J.-C. Marchon, *Inorg. Chim. Acta* **1994**, *215*, 203.
23 J. Telser, R. S. Drago, *Inorg. Chem.* **1984**, *23*, 3114.
24 F. D. Cukiernik, D. Luneau, J.-C. Marchon, P. Maldivi, *Inorg. Chem.* **1998**, *37*, 3698.
25 H. Miyasaka, R. Clérac, C. S. Campos-Fernández, K. R. Dunbar, *Inorg. Chem.* **2001**, *40*, 1663.
26 M. C. Barral, R. González-Prieto, R. Juménez-Aparicio, J. L. Priego, M. R. Torres, F. A. Urbanos, *Eur. J. Inorg. Chem.* **2003**, 2339.
27 G. Arribas, M. C. Barral, R. González-Prieto, R. Jiménez-Aparicio, J. L. Priego, M. R. Torres, F. A. Urbanos, *Inorg. Chem.* **2005**, *44*, 5770.
28 J. G. Norman, Jr., G. E. Renzoni, D. A. Case, *J. Am. Chem. Soc.* **1979**, *101*, 5256.
29 W.-Z. Chen, F. A. Cotton, N. S. Dalal, C. A. Murillo, C. M. Ramsey, T. Ren, X. Wang, *J. Am. Chem. Soc.* **2005**, *127*, 12691.
30 If the main contributor to the decrease of the magnetic moment is the ZFS effect, the following expressions for the magnetic susceptibility of $S = 3/2$ are applicable:

$$\chi_{\parallel} = \frac{Ng^2\beta^2}{k_B T} \frac{1 + 9e^{-2x}}{4(1 + e^{-2x})}, \tag{1}$$

$$\chi_{\perp} = \frac{Ng^2\beta^2}{k_B T} \frac{4 + \frac{3}{x}(1 - e^{-2x})}{4(1 + e^{-2x})}, \tag{2}$$

where x is $D/(k_B T)$ and D is the magnitude of the ZFS. The average molar magnetic susceptibility is given as follows:

$$\chi_{\text{total}} = \frac{\chi_{\parallel} + 2\chi_{\perp}}{3}. \tag{3}$$

The contributions of temperature-independent paramagnetism (TIP) and impurities as Ru(III) or Ru_2(III, III) species were excluded for simplicity, although those have been included in some cases of Ru_2(II, III) materials reported so far.
31 Using the mean-field approximation to treat the intermolecular interactions, the following definition of the susceptibility has been used:

$$\chi = \frac{\chi_{\text{total}}}{1 - \frac{2zJ}{Ng^2\mu_B^2}\chi_{\text{total}}},$$

where z is the number of neighboring molecules that are interacting with a molecule. See for example: a) B. E. Myers, L. Berger, S. Friedberg, *J. Appl. Phys.* **1969**, *40*, 1149. b) C. J. O'Connor, *Prog. Inorg. Chem.* **1982**, *29*, 203.
32 D. E. Richardson, H. Taube, *Inorg. Chem.* **1981**, *20*, 1278.
33 M. B. Robin, P. Day, *Adv. Inorg. Chem. Radiochem.* **1967**, *10*, 247.